




# The effect of repeat length on Marcal1-dependent single-strand annealing in *Drosophila*

Evan B. Dewey <sup>1,2</sup>, Julie Korda Holsclaw <sup>1</sup>, Kiyarash Saghaey<sup>3</sup>, Mackenzie E. Wittmer<sup>3</sup>, Jeff Sekelsky <sup>1,2,3,\*</sup>

<sup>1</sup>Integrative Program for Biological and Genome Sciences, University of North Carolina at Chapel Hill, Chapel Hill, NC 27599, USA

<sup>2</sup>Lineberger Comprehensive Cancer Center, University of North Carolina at Chapel Hill, Chapel Hill, NC 27599, USA

<sup>3</sup>Department of Biology, University of North Carolina at Chapel Hill, Chapel Hill, NC 27599, USA

\*Corresponding author: Integrative Program for Biological and Genome Sciences, University of North Carolina at Chapel Hill, Chapel Hill, NC 27599, USA.

Email: [sekelsky@unc.edu](mailto:sekelsky@unc.edu)

## Abstract

Proper repair of DNA double-strand breaks is essential to the maintenance of genomic stability and avoidance of genetic disease. Organisms have many ways of repairing double-strand breaks, including the use of homologous sequences through homology-directed repair. While homology-directed repair is often error free, in single-strand annealing homologous repeats flanking a double-strand break are annealed to one another, leading to the deletion of one repeat and the intervening sequences. Studies in yeast have shown a relationship between the length of the repeat and single-strand annealing efficacy. We sought to determine the effects of homology length on single-strand annealing in *Drosophila*, as *Drosophila* uses a different annealing enzyme (Marcal1) than yeast. Using an in vivo single-strand annealing assay, we show that 50 base pairs are insufficient to promote single-strand annealing and that 500–2,000 base pairs are required for maximum efficiency. Loss of Marcal1 generally followed the same homology length trend as wild-type flies, with single-strand annealing frequencies reduced to about a third of wild-type frequencies regardless of homology length. Interestingly, we find a difference in single-strand annealing rates between 500-base pair homologies that align to the annealing target either nearer or further from the double-strand break, a phenomenon that may be explained by Marcal1 dynamics. This study gives insights into Marcal1 function and provides important information to guide the design of genome engineering strategies that use single-strand annealing to integrate linear DNA constructs into a chromosomal double-strand break.

**Keywords:** DNA repair; DSB repair; annealing

## Introduction

Cellular DNA damage, particularly that caused by double-strand breaks (DSBs), must be properly cleared to maintain viability. DSBs arise from numerous intra- and extra-cellular sources, including external environmental chemical mutagens and ionizing radiation, as well as intracellular oxidative and replicative stress (Pfeiffer *et al.* 2000; Ciccia and Elledge 2010; Sage and Shikazono 2017). Left unrepaired, DSBs trigger apoptosis, and in improperly regulated cells aberrant repair can cause insertions, deletions, and translocations, leading to genomic instability and disease. Thus, it is critical for DSBs to be properly repaired to provide stability and avoid disease.

Cells have evolved robust mechanisms to repair DSBs accurately and avoid deleterious fates. Repair mechanisms are generally divided into 2 categories: nonhomologous end-joining (NHEJ) and homology-directed repair (HDR). While each strategy is effective in clearing DSB damage, each also has consequential trade-offs. Canonical NHEJ does not require the homologous chromosome or sister chromatid as a template, instead requiring minimal processing of DSB ends prior to ligating them (Chang *et al.* 2017). This process is fast, simple, and efficient but can frequently lead to small insertions and deletions.

HDR, if executed properly, provides benefits over NHEJ. Because HDR uses a homologous sequence as a template it can provide a largely error-free mechanism of repair. The cell commits to HDR over NHEJ by creating single-stranded DNA (ssDNA) tails with 3'-OH ends using specific exonucleases, a process called resection (reviewed in Cejka and Symington 2021). ssDNA tails are protected from degradation by replication protein A (RPA) before pursuing one of the many sub-pathways of HDR to complete repair. One such pathway is single-strand annealing (SSA), in which the ssDNA strands anneal to complementary sequence in one another and trim away any excess ssDNA flaps (Sugawara and Haber 1992; Rong and Golc 2003; Storici *et al.* 2006; Bhargava *et al.* 2016). As a result of the requirement for a large amount of complementary sequence, SSA occurs when a DSB is situated between direct repeats and is the major HDR pathway resulting in large deletions. In contrast to other HDR pathways, which generally have high fidelity, SSA necessarily generates a deletion.

Prior studies have identified proteins involved in SSA in fungi, invertebrates, and mammalian cell lines (reviewed in Bhargava *et al.* 2016; Vu *et al.* 2022). Studies in budding yeast found that loss of Rad52 or its paralog Rad59 resulted in near complete ablation

Received: September 24, 2022. Accepted: October 22, 2022

© The Author(s) 2022. Published by Oxford University Press on behalf of Genetics Society of America.

This is an Open Access article distributed under the terms of the Creative Commons Attribution License (<https://creativecommons.org/licenses/by/4.0/>), which permits unrestricted reuse, distribution, and reproduction in any medium, provided the original work is properly cited.

of SSA (Sugawara and Haber 1992; Ivanov et al. 1996; Sugawara et al. 2000). Rad52 binds ssDNA with strong affinity and can displace the ssDNA binding protein RPA to facilitate annealing between complementary sequences, an activity likely important to promoting SSA (Shinohara and Ogawa 1998; Grimme et al. 2010; Ma et al. 2017). RAD52 has also been implicated in SSA in mammalian cells, though its loss does not completely ablate SSA in these cells (Kelso et al. 2019).

While Rad52 functions in SSA in yeast and mammalian cells, it has been lost at several points in eukaryotic diversification, including in Dipteran insects (Sekelsky 2017). In *Drosophila*, Marcal1 is required for SSA (Korda Holsclaw and Sekelsky 2017). Biochemical studies of Marcal1 demonstrate annealing activity promoted through a HepA-related protein (HARP) domain (Yusufzai and Kadonaga 2008; Kassavetis and Kadonaga 2014), and thus, it seems likely that Marcal1 has the same SSA role in flies as Rad52 in yeast. The human ortholog, SMARCAL1, has similar activities (Coleman et al. 2000; Ghosal et al. 2011), though a role in SSA has not been reported.

To gain insight into how Marcal1 promotes SSA through its annealing activity, we asked how changing the length of available complementarity would affect SSA efficiency in both wild-type and *Marcal1* mutant flies. This question is also of interest because SSA can be used for CRISPR/Cas9-based genome editing to incorporate fragments into the *Drosophila* genome (Kanca et al. 2022). Demonstration of this approach employed a plasmid with 200 nt of flanking homology to either side of 2 Cas9 genomic targets. The plasmid was cut in vivo to generate a linear fragment. Understanding the effects of length of homology on SSA efficiency may improve the success of this approach.

Here, we show that efficiency of SSA in *Drosophila* is indeed dependent on the length of homology available, with 50 bp being insufficient and more than 500 bp being required for optimal SSA. The amount of resection required to expose complementary sequences used in SSA does not affect SSA efficacy when large amounts of homology are present in wild type, though smaller amounts do appear to be more sensitive to resection distance. In flies lacking Marcal1, SSA success is significantly reduced compared to wild type regardless of length of homology present. However, even in the complete absence of Marcal1, there is substantial residual SSA, suggesting the existence of another annealing enzyme.

## Materials and methods

### Cloning of P{wIw} constructs

Varying lengths of homology were made by reconstructing the P{wIw} construct used previously (Rong and Golic 2003; Wei and Rong 2007). We started with w+attB (previously deposited into AddGene, plasmid # 30326), which has a fully functional *white* gene under control of a basal *Hsp70Bb* promoter (*Hsp70Bb::white*; referred to as *mini-white*). We added a full-length, nonfunctional *mini-white* gene with truncated exon 1 (3.5 kb) and a 3' I-SceI site upstream of the functional *mini-white* in the form of two gBlocks (Integrated DNA Technologies). These incorporated restriction enzyme sites such that cleavage and relegation would delete various segments of the upstream *mini-white* gene sequence. Deleting between *HindIII* sites left 2 kb 5' homology; between 2 *NheI* sites left 2 kb 3' homology; between two *AvrII* left 500-bp 5' homology; between 2 *AgeI* sites left 500-bp 3' homology; and between two *MluI* sites left 50-bp 3' homology. The two gBlocks were added to the w+attB vector by InFusion cloning (Clontech/Takara) into the *HindIII* site. Once the full-length, nonfunctional 5' copy was

inserted, varying homologies described were created by cutting with a particular enzyme and ligating with T4 DNA ligase (New England Biolabs). All vectors were checked via Sanger sequencing to confirm proper amount/arrangement of upstream homology.

### *Drosophila* stocks

*Drosophila* stocks were kept at 25°C on standard cornmeal medium (Archon Scientific). Mutant alleles used in this article include *Marcal1<sup>kh1</sup>* (Korda Holsclaw and Sekelsky 2017) and *Marcal1<sup>del</sup>* (Baradaran-Heravi et al. 2012). Once all P{wIw} constructs were cloned, each was embryonically injected and integrated onto chromosome 3 via phiC31 integration into PBac{y+attP-3B}VK00031 (62E) (BestGene). Positive integrants were confirmed by expression of *mini-white* in a *y<sup>2</sup> w<sup>A</sup>* background. Integrants were balanced over TM6B and combined with *Marcal1<sup>kh1</sup>* mutants on chromosome 2.

### P{wIw} assay

The P{wIw} SSA repair assay was performed as described previously (Korda Holsclaw and Sekelsky 2017). Briefly, for each length/arrangement of homology, 4–5 *Marcal1<sup>kh1</sup>/CyO*; P{wIw}/TM6B virgin females were crossed to 3 *Marcal1<sup>del</sup>/CyO*; *Sb* P{*Hsp70Bb::I-SceI*}/TM6B males. One day later, first-instar larval progeny were heat-shocked at 37°C for 1 h to induce expression of I-SceI. Heat shock was repeated on the following day to ensure all first-instar larvae expressed I-SceI. Larvae were then allowed to develop to adulthood, and *Marcal1<sup>kh1</sup>/Marcal1<sup>del</sup>*; P{wIw}/*Sb* P{*Hsp70Bb::I-SceI*} males were collected. It should be noted that since the P{wIw} constructs are only present on 1 copy of the third chromosome, only 1 homolog is cut, and only intrahomolog or intersister (if present) recombination events are possible since there are no complementary sequences on the homologous chromosome. These males were then crossed 1 at a time to 4–5 *y<sup>2</sup> w<sup>A</sup>* virgin females for 3 days and then discarded. Progeny from these crosses were then scored for red or white eyes. To ensure that continued cutting with I-SceI did not occur throughout development, only *Sb<sup>+</sup>* progeny were scored. Two red-eyed and two white-eyed flies were collected from each vial for analysis. DNA from each collected fly was extracted for analysis of the cut site (in red-eyed flies) and the repair products (in white-eyed flies).

To assess whether maternally deposited Marcal1 was affecting SSA in the zygotic embryos' developing germlines, we additionally performed crosses with *Marcal1<sup>kh1</sup>/Marcal1<sup>del</sup>*; P{wIw}/TM6B females for 4 different homology lengths (3.5 kb, 2 kb 5', 500 bp 5' and 50 bp). We found no significant difference in white-eyed rates in males generated from this cross vs males generated from the initial cross with heterozygous mothers, indicating no detectable effect from maternally deposited Marcal1 on SSA (Supplementary Fig. 2).

### PCR analysis of red-eyed and white-eyed flies

To determine the cutting efficiency of I-SceI for each length/arrangement of homology, the area surrounding and including the cut site was amplified by PCR from 1 red-eyed fly per vial with forward primer 5'-AGCGGATAACAATTTACACACAGG-3' (M13R) and reverse primer 5'-AGCGGATAACAATTTACACACAGG-3' (SSA\_R) (see Supplementary Fig. 1 for cutting efficiency). PCR products were subjected to cutting with I-SceI (New England Biolabs) for 1 h at 37°C and then run on an agarose gel. If amplified DNA was uncut by I-SceI, this indicates that the I-SceI site was likely cut in vivo and then mutated/deleted through end-joining (NHEJ). If amplified DNA was cut by I-SceI, this indicates that the I-SceI site was likely not cut in vivo or less likely joined without mutation/deletion by

NHEJ. DNA successfully cut by I-SceI could not be distinguished between uncut and perfect NHEJ.

To determine the type of repair that occurred in white-eyed flies for length/arrangement homology, the area flanking nonfunctional 5' and functional 3' *mini-w* genes was amplified by PCR for 1 white-eyed fly per vial with forward primer 5'-GTTCGCTCA AATGGTTCGGA-3' (pwlw\_I-SceI\_L) and reverse primer 5'-TCGCG ATGTGTTCACTTTGT-3' (pwlw\_I-SceI\_R). PCR products were then run on a gel and repair product type determined by size. Each length/arrangement of homology has a particular sized band predicted for an SSA repair product (meaning that SSA likely occurred *in vivo*), with larger and smaller bands classified as "non-SSA repair products," meaning that these flies had a type of repair that caused a deletion into the functional white gene but not due to repair by SSA.

## Statistical analyses

Statistical analyses were conducted in Prism 9.4 (GraphPad). Specific tests used are given in figure legends.

## Results

### SSA effectiveness is dependent on the length of homology present

To determine how length of homology affects efficiency of SSA in *Drosophila*, we built a modified  $P\{wIw\}$  assay (Rong and Golic 2003). In the original  $P\{wIw\}$ , 2 copies of the *mini-white* gene are inserted in tandem with an I-SceI cut site in the middle (Fig. 1a, top). The copy downstream (3') of the I-SceI cut site is functional, while the upstream (5') copy is nonfunctional due to deletion of the promoter and part of the first exon. To perform the assay, I-SceI is expressed via heat shock in the developing germline of males heterozygous for the insertion of  $P\{wIw\}$  on the third chromosome, and repair events recovered in progeny (Fig. 1, b–e). In previous studies, about 90% of progeny had cleavage and repair by SSA, suggesting that strand invasion and repair off the homologous chromosome is rare. Our modified assays retain this high I-SceI cleavage efficacy, with 89.9% cleavage across all wild-type homologies and 82.0% cleavage across all *Marcal1* homologies (Supplementary Fig. 1).

If the DSB is repaired by canonical NHEJ, resulting progeny will have red eyes (Fig. 1b). The I-SceI site in this case is often mutated due to the mutagenic nature of NHEJ, as nonmutated sites can be re-cut and re-repaired until a mutated, uncuttable outcome is produced (Fig. 1b). Red eyes can also result from DNA polymerase theta-mediated end-joining (TMEJ), a process that anneals microhomologies near the ends of resected DNA strands (Fig. 1c) (Chan et al. 2010; Carvajal-Garcia et al. 2020). If resection on both sides of the break uncovers complementarity between the truncated upstream and full-length downstream *mini-white* genes, the repair product lacks a promoter and the first exon, resulting in progeny in white eyes among the progeny that inherit this SSA repair product (Fig. 1d). White eyes may also result from larger deletions into the promoter or coding sequence of the downstream *mini-white*; such deletions can be detected by PCR and sequencing (Fig. 1e).

To better elucidate *Marcal1*-based SSA mechanisms in *Drosophila*, we inserted  $P\{wIw\}$  constructs with upstream various nonfunctional *mini-white* fragments, creating 5 distinct versions (Fig. 1a). We varied whether upstream homology was taken from the 5' or 3' portion of the *mini-white* gene, while keeping the distance from the downstream functional *mini-white* the same

(Fig. 1a, yellow boxes). With homologies taken from the 3' part of the gene, more resection into the downstream *mini-white* gene is needed to expose complementary sequences. We hypothesized that this increased resection requirement and/or the different flap sizes generated by annealing these differing homologies might provide an additional constraints to effective SSA.

In wild-type flies, the percentage of white-eyed progeny (indicating likely SSA repair) was not significantly different between full-length  $P\{wIw\}$  (3.5 kb of homology; 90.8%) and 2 kb of homology from either the 5' (90.1%) or 3' (89.0%) end of the gene (Fig. 2, a and b and Table 1).

However, when homology from the downstream functional *mini-white* was reduced to 500 bp from either the 5' or 3' portion, there was a significant decrease in the number of white-eyed progeny compared to both full-length and 2-kb homologies (59.3% and 70.1%, respectively,  $P < 0.0001$ ), indicating reduced SSA (Fig. 2, a and b and Table 1). Contrary to our hypothesis that 3' homology might be additionally constraining on SSA due to the additional resection required, the opposite appeared to be true for the 500-bp homologies, with the 3' 500-bp homology producing significantly more white-eyed progeny compared to the 5' counterpart (Fig. 2, a and b and Table 1,  $P < 0.001$ ). Finally, when we reduced the amount of 5' homology to 50 bp (from only the 3' portion of the nonfunctional *mini-white* gene), we saw a significant decrease in white-eyed progeny compared to all other homology lengths (8.3%,  $P < 0.0001$  for each comparison), indicating that 50 bp is below the homology threshold necessary for efficient SSA in this assay.

While most of the white-eyed progeny in the  $P\{wIw\}$  assay result from SSA repair, white eyes may also result from non-SSA deletions into the functional *mini-white* gene (Fig. 1e). To quantify this, we analyzed repair products in progeny. Because repair in the proliferating germline can result in multiple progeny from a single event, we assured independence of repair events by analyzing just 1 white-eyed offspring per vial, for a total of about 30 flies per experiment. Across all homology lengths except 50 bp (excluded as most vials did not have white-eyed progeny), SSA was the predominant form of repair (Fig. 3a); for longer homologies (3.5 kb, 2 kb 5', and 2 kb 3'), all white-eyed flies resulted from SSA (Fig. 3, b and c). For the 500-bp homologies, we detected some non-SSA products, particularly in case of the 5' homology (13.3% non-SSA; Fig. 3d), suggesting that SSA repair efficacy in *Drosophila* begins to diminish between 2 kb and 500 bp of homology. When we further multiply the white-eyed progeny for each condition by the percentage of SSA PCR products, we can obtain the true rate of SSA per condition (SSA rate, Table 1). While SSA rates for homologies of 2 kb and above remain unchanged from the percentage of white-eyed progeny, as all white-eyed flies obtained yielded SSA products, we did see a modest decrease when comparing the percentage of white-eyed flies to the SSA rates for both 500-bp homologies, reflecting a more accurate rate of SSA for these conditions (Table 1). Last, for the 50-bp 3' homology, we see that in vials with white-eyed flies, almost all repair products are non-SSA (90.9%, Supplementary Fig. 3), further indicating that 50 bp is not enough homology to perform SSA efficiently in *Drosophila*.

### Loss of *Marcal1* reduces SSA irrespective of homology length

We next asked whether differing lengths of homology affected the efficacy of SSA in a *Marcal1* mutant background. Regardless of homology length, *Marcal1* mutants produced significantly

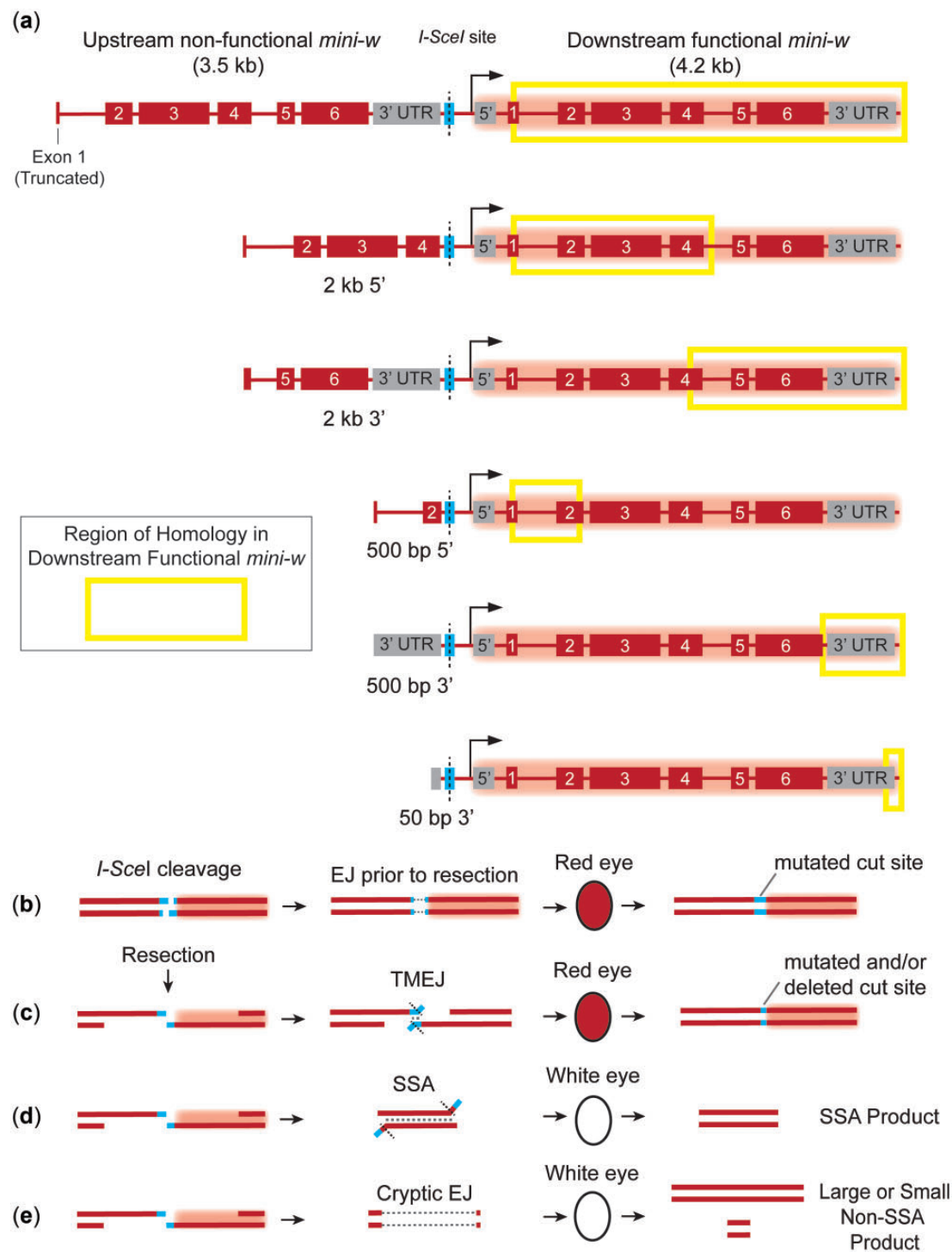


**Fig. 1.**  $P\{wIw\}$  assay design and outcomes. a) Homologies used in the  $P\{wIw\}$  assay. The original assay (Rong and Golic 2003) uses a nonfunctional *mini-white* gene with part of exon 1 deleted. This is upstream (5') of the *I-SceI* site. Our assay uses different upstream homology lengths corresponding to different regions of the functional, downstream (3') *mini-w* gene (yellow boxes). b–e) Outcomes of the assay. b) Imprecise nonhomologous end-joining (NHEJ/EJ) results in a mutated *I-SceI* cut site and leads to a red eye in progeny. c) Resection followed by DNA polymerase TMEJ results in a mutated or deleted *I-SceI* cut site, preventing further cutting and resulting in a red eye in progeny. d) Resection followed by SSA results in a distinct deletion for each homology class (SSA product) and white eyes in progeny. e) Some deletions are larger than expected by canonical NHEJ or TMEJ; we refer to these as cryptic end-joining since their origins have not been determined.

fewer white-eyed progeny compared to wild type ( $P < 0.05$  for each, Table 1 and Supplementary Fig. 4). Our results also show a decrease of 41% for the assay with 3.5-kb homology when *Marcal1*

is mutated (Fig. 2, c and d and Table 1). We speculated the effects of *Marcal1* loss might become more severe as homology lengths were reduced; however, we found a 40–50% reduction in



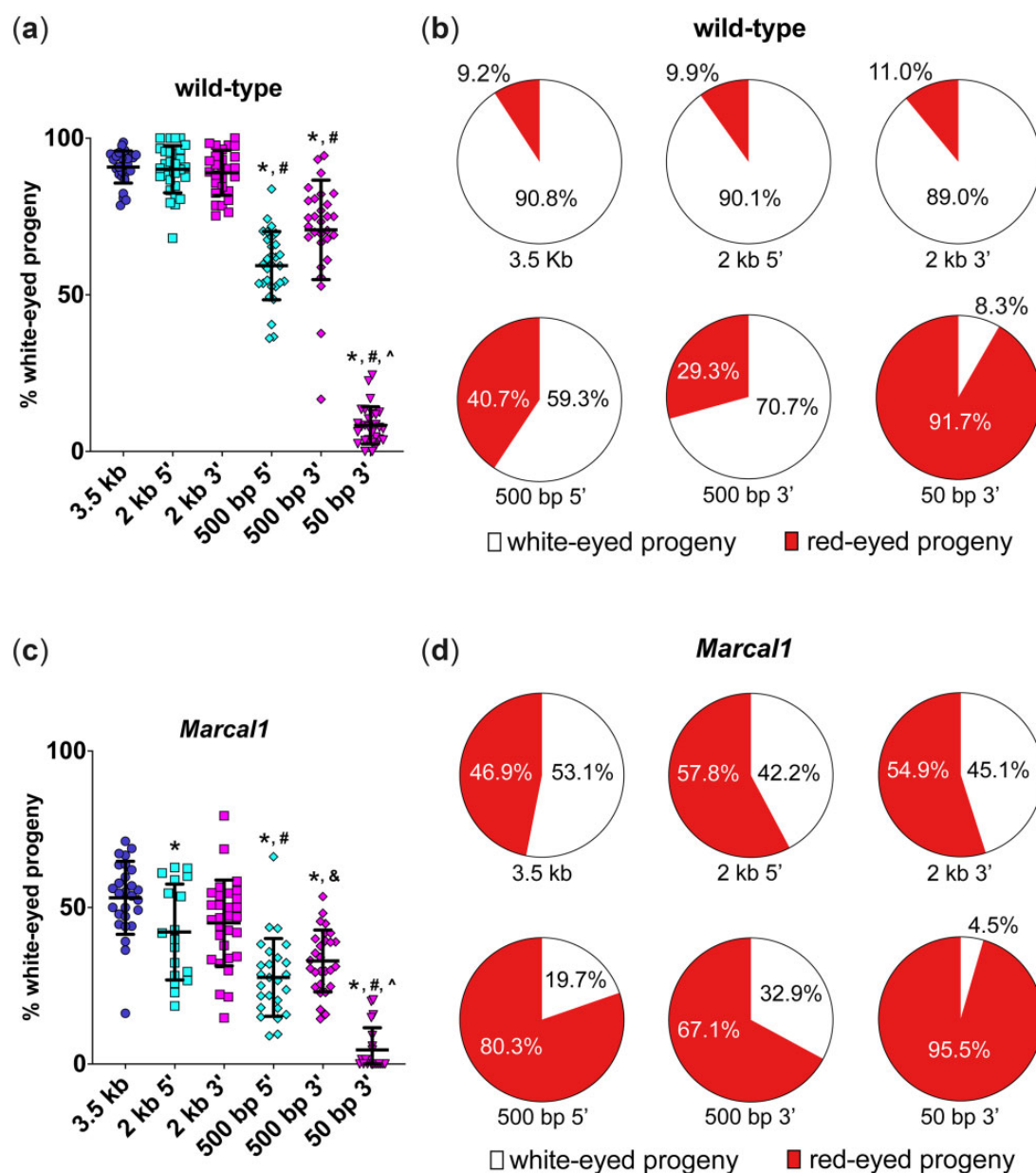


**Fig. 2.** Length of homology affects SSA efficiency in wild-type and *Marcal1* mutant flies. a) Percent of total progeny with white eyes in wild-type *P{wIw}* crosses. \* $P < 0.05$  vs 3.5-kb homology, # $P < 0.05$  vs 2-kb homology (5' and 3'),  $\bar{P} < 0.05$  vs 500-bp homology (5' and 3'), \*\*\* $P < 0.0001$  between 500 bp 5' and 500 bp 3' (ANOVA with Tukey's post hoc test). b) Pie charts showing the white-eye vs red-eye progeny for each wild-type assay. While the 3.5- and 2-kb homologies provide good templates for SSA (top row), as homology length is reduced, SSA efficiency diminishes (bottom row). c) Percent of total progeny with white eyes in *Marcal1 P{wIw}* crosses. \* $P < 0.05$  vs 3.5-kb homology, # $P < 0.05$  vs 2-kb homology (5' and 3'),  $\bar{P} < 0.05$  vs 2-kb 3' homology, ^ $P < 0.05$  vs 500-bp homology (5' and 3') (ANOVA with Tukey's post hoc test). For 50 bp 3',  $n = 1,286$  progeny; other  $n$  values are in Table 1. d) Pie charts showing the white-eyed vs red-eyed progeny for each assay in *Marcal1* mutant flies.

**Table 1.** Comparisons of SSA frequencies between wild-type and *Marcal1* mutant flies.

Assay	Wild type			Marcal1 mutant			Marcal1/WT
	White eyes	SSA PCR	SSA rate	White eyes	SSA PCR	SSA rate	
3.5 kb	91	100	91	53	75	40	0.34
2 kb 5'	90	100	90	42	53	22	0.24
2 kb 3'	89	100	89	45	65	29	0.33
500 bp 5'	59	87	51	28	80	22	0.43
500 bp 3'	71	97	68	33	64	21	0.31

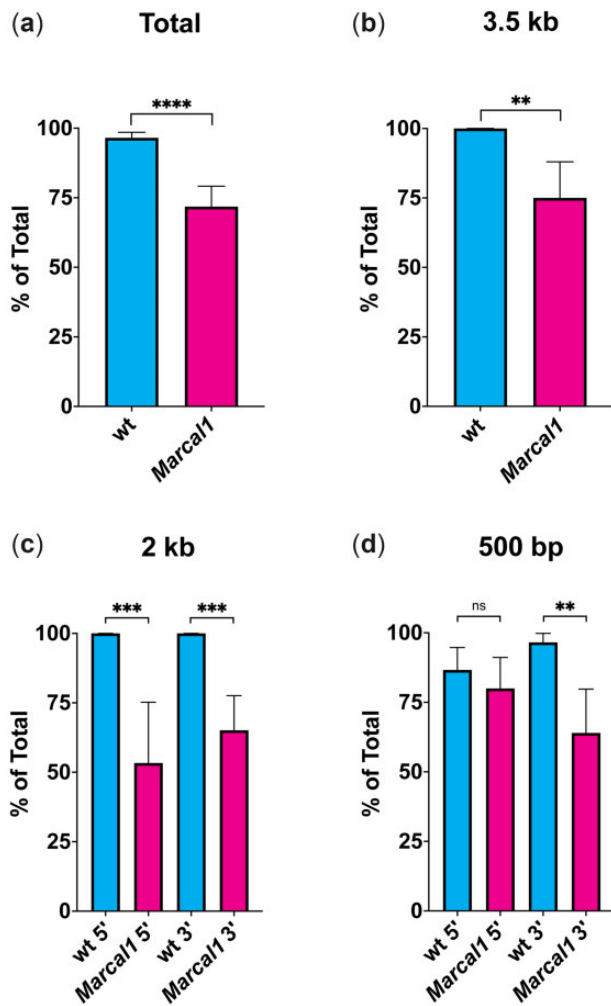


**Fig. 3.** Molecular analysis of white-eyed progeny. In white-eyed progeny, the repaired region was amplified by PCR to determine whether region was repaired by SSA, producing a distinct product size or cryptic EJ, producing a larger or smaller product. Data from wild-type flies and *Marcal1* mutants were compared by Fisher's exact test. a) Summed data from all assays except 50 bp.  $n = 144$  for wt;  $n = 117$  for *Marcal1*; \*\*\*\* $P < 0.0001$ . b) 3.5-kb homology.  $n = 29$  for wild type, 24 for *Marcal1*; \*\* $P < 0.01$ . c) 2-kb 5' and 3' homologies. For 5'  $n = 30$  for wild type, 15 for *Marcal1*; for 3'  $n = 26$  for wild type, 43 for *Marcal1*; \*\*\* $P < 0.001$ . d) 500-bp 5' and 3' homologies. For 5'  $n = 30$  for wild type, 25 for *Marcal1*; for 3'  $n = 29$  for wild type, 25 for *Marcal1*; n.s.,  $P = 0.7165$ ; \*\* $P < 0.01$ .

white-eyed progeny from wild type regardless of the amount of homology present (Fig. 2, c and d and Table 1). Overall, *Marcal1* mutants follow the same trend as wild type, with decreasing homology yielding decreasing amounts of white-eyed progeny (Fig. 2, c and d and Table 1).

### SSA repair events are less prevalent in *Marcal1* white-eyed progeny

When initially examining the role of *Marcal1* in SSA, Korda Holsclaw and colleagues found that while the majority of white-eyed progeny from wild-type flies resulted from SSA repair, many of the white-eyed progeny in *Marcal1* mutants resulted from non-SSA deletions into the functional *mini-white* gene. In agreement with this prior work, we found that the percentage of white-eyed progeny that resulted from SSA repair was significantly different between wild-type and *Marcal1* mutants (excluding 50-bp 3'

homology) across all homology amounts/lengths (96.5% and 71.8%, respectively; Fig. 3a and Table 1, SSA products).

When examining the percentage of white-eyed flies with SSA products at differing lengths of homology, *Marcal1* mutant progeny do not follow the trend established in wild-type flies. While there is a decrease in the amount of SSA products when reducing homology from 3.5 to 2 kb 5' and 3' (Fig. 3, b and c), SSA products appear to remain the same or even increase when comparing the larger homologies (3.5 and 2 kb) to the 500-bp homologies (Fig. 3, b and c vs Fig. 3d and Table 1). When we multiply the percentage of white-eyed progeny by the percentage of SSA products to obtain the true SSA rate, we observe a decrease across all homologies (Table 1). Dividing the true SSA rates from *Marcal1* mutants by those from wild-type flies shows that the decrease in SSA is stronger in *Marcal1* flies when compared to the difference only in white-eyed progeny rates, varying from 44% to as low as 24% of wild type depending on condition (*Marcal1*/WT, Table 1). Together, these results indicate that the effects of loss of *Marcal1* on SSA are not strongly dependent on the length of homology.

## Discussion

### Homology amounts affect SSA

Here, we demonstrate that homology length affects SSA in *Drosophila*. This agrees with previous studies in yeast (Sugawara and Haber 1992; Sugawara et al. 2000), and in human cell lines (Rothenberg et al. 2008; Kelso et al. 2019), although there are some differences across organisms in the threshold of homology required for SSA outcomes. Compared with our study, in which we begin to see a decrease in SSA efficacy in wild type between 2 kb and 500 bp, studies in yeast find a lower threshold, with this decrease starting between 905 and 415 bp when *Rad52* is lost (Sugawara and Haber 1992), or between 415 and 235 bp when *Rad59* is lost (Sugawara et al. 2000). This is less clear in human studies, as the variable lengths used are much smaller than in these and prior yeast experiments, topping out with homology lengths of 50 bp (Rothenberg et al. 2008) or 200 bp (Kelso et al. 2019). Whether higher amounts of homology yield better SSA rates in these contexts remains to be seen. Differences in the distances between repeats and their arrangements may also be a factor, with SSA in *rad52* mutants diminished as distance between repeats increases (Mendez-Dorantes et al. 2018). Furthermore, SSA in *rad52* mutants was observed with very large repetitive sequences (*rDNA* [0.9–1.8 Mb] and *CUP1* tandem repeats [36 kb]), indicating that for such sequences, a different mechanism may exist (Ozenberger and Roeder 1991). Regardless, our work and others point to a homology threshold to efficiently carry out SSA. Factors involved in SSA may need a certain length to properly anneal repetitive sequence, with lower homology amounts not annealing as well as higher homology amounts. Stability gained through annealing could then allow for the accumulation of other SSA factors, such as endonucleases to cleave ssDNA flaps.

Why do organisms vary in their homology threshold amounts? This may be dependent on the primary annealing enzyme(s) involved in SSA; *Drosophila* *Marcal1* may require longer stretches of complementarity than *Rad52* in yeast and mammals. It is also possible that other SSA factors contribute to the differences.

We noted a significant difference in SSA repair between the 5' 500-bp repeat and 3' 500-bp repeat. GC content is similar, with 42% GC for 5' 500-bp repeat compared to 40% for the 3' 500-bp repeat. In addition, secondary structure analysis of ssDNA does not suggest a large discrepancy between free energy ( $\Delta G$ ) of predicted

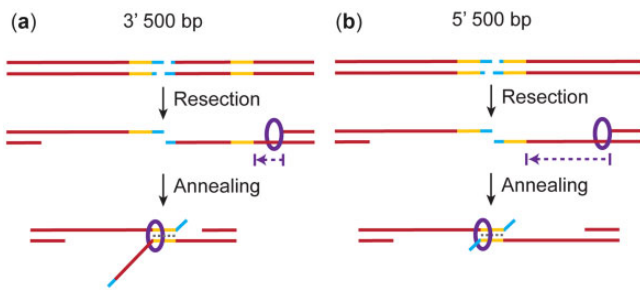


**Fig. 4.** Possible mechanism for Marcal1 SSA based on differences between 5' and 3' 500-bp homologies. a) Proposed Marcal1 mechanism for the 3' 500-bp homology. Upon I-SceI cutting (blue) and 5' resection, Marcal1 (purple ring) localizes to the ssDNA–dsDNA interface created by resection. Marcal1 translocates along the ssDNA (indicated by purple arrow) until it finds a region of complementarity (yellow) and promotes annealing. b) Proposed Marcal1 mechanism for the 5' 500-bp homology. Marcal1 (purple ring) localizes to the ssDNA–dsDNA interface created by resection and then translocates (purple arrow) toward the initial cut site (blue). However, since the 5' 500-bp homology (yellow) of the functional *mini-white* gene is further from the ssDNA–dsDNA resection end point, Marcal1 must translocate a greater distance to reach homology and a higher probability of dissociation before reaching the region of complementarity. This may provide a longer window during which DNA polymerase theta can engage the ends to carry out TMEJ, resulting in a reduction in the SSA outcome.

secondary structure formation for 5' 500 vs 3' 500 bp,  $-124.3$  and  $-96.9$  kcal/mol, respectively. It is possible that the larger flap of ssDNA generated by annealing the 3' 500-bp segments may be more favorable for cleavage (Fig. 4a). The enzyme(s) executing this cleavage have yet to be identified in *Drosophila*, but Mei-9 and Mus312, which are orthologous to Rad1 (the catalytic subunit) and Slx4 (a scaffold protein) that are used in budding yeast (Fishman-Lobell and Haber 1992; Toh et al. 2010), are not required (Wei and Rong 2007). Conversely, TMEJ may be favorable than SSA when the flap is shorter, as with the 5' 500-bp segment. This could explain why more red-eyed flies are present in experiments with the 5' 500-bp repeat, as a TMEJ mechanism would not be predicted to cause deletions into the downstream functional *mini-white* gene (see below, Carvajal-Garcia et al. 2020).

Another possibility is that there is a preference to anneal repeats closer to the ssDNA–dsDNA interface created by resection. Based on high efficiency of the original  $P\{wIw\}$  assay, resection occurs at least 3.5 kb from the break site. By this mechanism, there would be more ssDNA between where the repeats anneal and the ssDNA–dsDNA interface for the 5' 500-bp repeat, compared to less for the 3' 500-bp repeat (Fig. 4). This “interstitial” or “intervening” ssDNA could be more taxing for the cell to deal with, as there would be more of a ssDNA gap to fill following SSA with the 5' 500-bp repeat vs the 3' 500-bp repeat, making the 3' 500-bp repeat more efficient.

A preference to anneal repeats closer to the ssDNA–dsDNA interface is an attractive model for *Drosophila* because of the binding characteristics of Marcal1. In vitro studies found that human SMARCAL1 and *Drosophila* Marcal1 bind to fork structures, which have an ssDNA–dsDNA interface, with higher affinity than to ssDNA and dsDNA (Yusufzai and Kadonaga 2008; Kassavetis and Kadonaga 2014). If Marcal1 is preferentially recruited to ssDNA–dsDNA interfaces, the start of the 3' 500-bp ssDNA that would be annealed is closer to such an interface than for the 5' 500-bp ssDNA (Fig. 4, a and b). This would lower the ssDNA distance Marcal1 would need to traverse before annealing could be initiated, thereby favoring SSA. This preference would diminish with larger homologies used in our assays, as longer upstream

homologies, even those matching the 5' end of the downstream copy, decrease the distance between the ssDNA–dsDNA interface and annealing start site.

This mechanism would contrast Marcal1 with Rad52 function in several ways. First, each differs in how it binds to DNA. While Marcal1 has a preference to bind to ssDNA–dsDNA interfaces (Yusufzai and Kadonaga 2008; Kassavetis and Kadonaga 2014), yeast and human Rad52 has been shown to prefer ssDNA over ssDNA–dsDNA interfaces (Shinohara and Ogawa 1998; Navadgi et al. 2003; Rossi et al. 2021). Second, both proteins would facilitate the annealing of homologous repeats differently. Rad52 forms oligomeric ring structures to bind ssDNA, with the rings then aggregating along the ssDNA (Shinohara and Ogawa 1998; Van Dyck et al. 1998; Stasiak et al. 2000; Ranatunga et al. 2001). The rings then interact with one another on opposing strands to facilitate annealing without the need to hydrolyze ATP (Ranatunga et al. 2001; Kagawa et al. 2008; Saotome et al. 2018). This contrasts with prior work in *Drosophila*, showing that SSA was affected by the mutation of the Marcal1 ATP-binding pocket, suggesting that Marcal1 needs to traverse DNA to facilitate annealing (Korda Holsclaw and Sekelsky 2017).

### Loss of Marcal1 decreases SSA repair rate vs wild type, regardless of homology length

Regardless of the amount of homology or the location of homology (5' vs 3'), mutation of *Marcal1* decreases SSA repair rates to between 56% and 76% vs wild type depending on homology (Fig. 3 and Table 1). This agrees with previous studies assaying *Marcal1* in SSA with full-length repeats in the  $P\{wIw\}$  assay (Korda Holsclaw and Sekelsky 2017), which saw a roughly 50% decrease (93.0% white-eyed progeny for wild type vs 44.6% for *Marcal1*). In both the presence and absence of *Marcal1*, 50 bp remains insufficient to carry out SSA, and maximal SSA frequency is achieved between 500 and 2,000 bp. This result suggests that *Drosophila* has other SSA annealing enzymes.

### Deletion frequency is increased in *Marcal1* mutants

Among the white-eyed progeny of *Marcal1* mutants, it was interesting to note that more non-SSA deletions were obtained. How might these deletions be facilitated? Canonical NHEJ can involve resection that requires the endonuclease Artemis (Biehs et al. 2017); however, *Drosophila* lacks an ortholog of this protein. While there is evidence for end processing in an NHEJ context in *Drosophila* (Bozas et al. 2009), there have yet to be any genes identified that might participate in this process. A 2007 screen by Wei and Rong (2007) did see some large deletions when NHEJ components (specifically *lig4*) were mutated in the  $P\{wIw\}$  assay. They suggested that it could be that ends are more susceptible to degradation when NHEJ components are mutated.

TMEJ is also a potential explanation for the increased deletions. However, the microhomology search extends only 15–20 nt from each end of the DSB, resulting in deletions of 34–40 bp (Carvajal-Garcia et al. 2020; Carvajal-Garcia et al. 2021). Given there are approximately 620 bp between the I-SceI cut site and the downstream functional *white* gene regardless of homology length in our assay, this would mean TMEJ deletions would likely not affect the functional *white* gene. It is therefore unlikely that TMEJ explains the large non-SSA deletions we observed among white-eyed progeny. It has been proposed that 3' ssDNA can be lost by the 3'–5' exonucleolytic function of DNA polymerase delta before polymerase theta can be engaged (Carvajal-Garcia et al. 2020; Carvajal-Garcia et al. 2021). This could explain some of the large

deletions we observed, though this would be difficult to test because it would require a 3′–5′ exonuclease separation-of-function allele of DNA polymerase delta that retains the essential replication functions of the protein. Finally, loss of RPA coating due to inefficient annealing may also play a role in generating deletions, as a recent study proposed unstable RPA could cause resected ssDNA to form secondary structures (e.g. intrastrand hairpins) susceptible to structure-specific endonucleases, resulting in aborted repair and large deletions (Ruff et al. 2016).

## SSA as a tool in CRISPR/Cas9 genome engineering in *Drosophila*

Kanca et al. (2022) showed that SSA can be used for CRISPR/Cas9 genome engineering in *Drosophila*. Although these authors achieved success with only 200bp of homology on each side of the DSB our work suggests that increasing this will enhance the success of integration, yielding more efficient gene edits per round of embryonic injections. Further studies can define the optimum conditions for CRISPR SSA integration that balance the needs of homology vs synthesis costs.

## Data availability

Plasmids, *Drosophila* stocks, and sequences are available upon request. The authors affirm that all data necessary for confirming the conclusions of the article are present within the article, figures, and table.

[Supplemental material](#) is available at GENETICS online.

## Acknowledgments

We thank members of the Sekelsky lab for helpful comments on the article.

## Funding

This work was supported by a grant from the National Institute of General Medical Sciences to JS under award 1R35GM118127. EBD was supported in part by a grants from the National Cancer Institute (T32 CA217824).

## Conflicts of interest

None declared.

## Literature cited

- Baradaran-Heravi A, Cho KS, Tolhuis B, Sanyal M, Morozova O, Morimoto M, Elizondo LI, Bridgewater D, Lubieniecka J, Beirnes K, et al. Penetration of biallelic SMARCAL1 mutations is associated with environmental and genetic disturbances of gene expression. *Hum Mol Genet.* 2012;21(11):2572–2587.
- Bhargava R, O Onyango D, Stark JM. Regulation of single-strand annealing and its role in genome maintenance. *Trends Genet.* 2016;32(9):566–575.
- Biehs R, Steinlage M, Barton O, Juhász S, Künzel J, Spies J, Shibata A, Jeggo PA, Löbrich M. DNA double-strand break resection occurs during non-homologous end joining in G1 but is distinct from resection during homologous recombination. *Mol Cell.* 2017;65(4):671–684.e5.
- Bozas A, Beumer KJ, Trautman JK, Carroll D. Genetic analysis of zinc-finger nuclease-induced gene targeting in *Drosophila*. *Genetics.* 2009;182(3):641–651.
- Carvajal-Garcia J, Cho J-E, Carvajal-Garcia P, Feng W, Wood RD, Sekelsky J, Gupta GP, Roberts SA, Ramsden DA. Mechanistic basis for microhomology identification and genome scarring by polymerase theta. *Proc Natl Acad Sci USA.* 2020;117(15):8476–8485.
- Carvajal-Garcia J, N Crown K, Ramsden DA, Sekelsky J. DNA polymerase theta suppresses mitotic crossing over. *PLoS Genet.* 2021;17(3):e1009267.
- Cejka P, Symington LS. DNA end resection: mechanism and control. *Annu Rev Genet.* 2021;55:285–307.
- Chan SH, Yu AM, McVey M. Dual roles for DNA polymerase theta in alternative end-joining repair of double-strand breaks in *Drosophila*. *PLoS Genet.* 2010;6(7):e1001005.
- Chang HHY, Pannunzio NR, Adachi N, Lieber MR. Non-homologous DNA end joining and alternative pathways to double-strand break repair. *Nat Rev Mol Cell Biol.* 2017;18(8):495–506.
- Ciccio A, Elledge SJ. The DNA damage response: making it safe to play with knives. *Mol Cell.* 2010;40(2):179–204.
- Coleman MA, Eisen JA, Mohrenweiser HW. Cloning and characterization of HARP/SMARCAL1: a prokaryotic HepA-related SNF2 helicase protein from human and mouse. *Genomics.* 2000;65(3):274–282.
- Fishman-Lobell J, Haber JE. Removal of nonhomologous DNA ends in double-strand break recombination: the role of the yeast ultraviolet repair gene RAD1. *Science.* 1992;258(5081):480–484.
- Ghosal G, Yuan J, Chen J. The HARP domain dictates the annealing helicase activity of HARP/SMARCAL1. *EMBO Rep.* 2011;12(6):574–580.
- Grimme JM, Honda M, Wright R, Okuno Y, Rothenberg E, Mazin AV, Ha T, Spies M. Human Rad52 binds and wraps single-stranded DNA and mediates annealing via two hRad52-ssDNA complexes. *Nucleic Acids Res.* 2010;38(9):2917–2930.
- Ivanov EL, Sugawara N, Fishman-Lobell J, Haber JE. Genetic requirements for the single-strand annealing pathway for double-strand break repair in *Saccharomyces cerevisiae*. *Genetics.* 1996;142(3):693–704.
- Kagawa W, Kagawa A, Saito K, Ikawa S, Shibata T, Kurumizaka H, Yokoyama S. Identification of a second DNA binding site in the human Rad52 protein. *J Biol Chem.* 2008;283(35):24264–24273.
- Kanca O, Zirin J, Hu Y, Tepe B, Dutta D, Lin WW, Ma L, Ge M, Zuo Z, Liu LP, et al. An expanded toolkit for *Drosophila* gene tagging using synthesized homology donor constructs for CRISPR-mediated homologous recombination. *eLife.* 2022;11:e76077.
- Kassavetis GA, Kadonaga JT. The annealing helicase and branch migration activities of *Drosophila* HARP. *PLoS One.* 2014;9(5):e98173.
- Kelso AA, Lopezcolorado FW, Bhargava R, Stark JM. Distinct roles of RAD52 and POLQ in chromosomal break repair and replication stress response. *PLoS Genet.* 2019;15(8):e1008319.
- Korda Holsclaw J, Sekelsky J. Annealing of complementary DNA sequences during double-strand break repair in *Drosophila* is mediated by the ortholog of SMARCAL1. *Genetics.* 2017;206(1):467–480.
- Ma CJ, Kwon Y, Sung P, Greene EC. Human RAD52 interactions with replication protein A and the RAD51 presynaptic complex. *J Biol Chem.* 2017;292(28):11702–11713.
- Mendez-Dorantes C, Bhargava R, Stark JM. Repeat-mediated deletions can be induced by a chromosomal break far from a repeat, but multiple pathways suppress such rearrangements. *Genes Dev.* 2018;32(7–8):524–536.



- Navadgi VM, Dutta A, Rao BJ. Human Rad52 facilitates a three-stranded pairing that follows no strand exchange: a novel pairing function of the protein. *Biochemistry*. 2003;42(51):15237–15251.
- Ozenberger BA, Roeder GS. A unique pathway of double-strand break repair operates in tandemly repeated genes. *Mol Cell Biol*. 1991; 11(3):1222–1231.
- Pfeiffer P, Goedecke W, Obe G. Mechanisms of DNA double-strand break repair and their potential to induce chromosomal aberrations. *Mutagenesis*. 2000;15(4):289–302.
- Ranatunga W, Jackson D, Lloyd JA, Forget AL, Knight KL, Borgstahl GE. Human RAD52 exhibits two modes of self-association. *J Biol Chem*. 2001;276(19):15876–15880.
- Rong YS, Golic KG. The homologous chromosome is an effective template for the repair of mitotic DNA double-strand breaks in *Drosophila*. *Genetics*. 2003;165(4):1831–1842.
- Rossi MJ, DiDomenico SF, Patel M, Mazin AV. RAD52: paradigm of synthetic lethality and new developments. *Front Genet*. 2021;12: 780293.
- Rothenberg E, M Grimme J, Spies M, Ha T. Human Rad52-mediated homology search and annealing occurs by continuous interactions between overlapping nucleoprotein complexes. *Proc Natl Acad Sci USA*. 2008;105(51):20274–20279.
- Ruff P, Donnianni RA, Glancy E, Oh J, Symington LS. RPA stabilization of single-stranded DNA is critical for break-induced replication. *Cell Rep*. 2016;17(12):3359–3368.
- Sage E, Shikazono N. Radiation-induced clustered DNA lesions: repair and mutagenesis. *Free Radic Biol Med*. 2017;107:125–135.
- Saotome M, Saito K, Yasuda T, Ohtomo H, Sugiyama S, Nishimura Y, Kurumizaka H, Kagawa W. Structural basis of homology-directed DNA repair mediated by RAD52. *Science*. 2018;359:50–62.
- Sekelsky J. DNA repair in *Drosophila*: mutagens, models and missing genes. *Genetics*. 2017;205(2):471–490.
- Shinohara A, Ogawa T. Stimulation by Rad52 of yeast Rad51-mediated recombination. *Nature*. 1998;391(6665):404–407.
- Stasiak AZ, Larquet E, Stasiak A, Müller S, Engel A, Van Dyck E, West SC, Egelman EH. The human Rad52 protein exists as a heptameric ring. *Curr Biol*. 2000;10(6):337–340.
- Storici F, R Snipe J, Chan GK, A Gordenin D, Resnick MA. Conservative repair of a chromosomal double-strand break by single-strand DNA through two steps of annealing. *Mol Cell Biol*. 2006;26(20):7645–7657.
- Sugawara N, Haber JE. Characterization of double-strand break-induced recombination: homology requirements and single-stranded DNA formation. *Mol Cell Biol*. 1992;12(2):563–575.
- Sugawara N, Ira G, Haber JE. DNA length dependence of the single-strand annealing pathway and the role of *Saccharomyces cerevisiae* RAD59 in double-strand break repair. *Mol Cell Biol*. 2000; 20(14):5300–5309.
- Toh GW-L, Sugawara N, Dong J, Toth R, Lee SE, Haber JE, Rouse J. Mec1/Tel1-dependent phosphorylation of Slx4 stimulates Rad1-Rad10-dependent cleavage of non-homologous DNA tails. *DNA Repair (Amst)*. 2010;9(6):718–726.
- Van Dyck E, Hajibagheri NM, Stasiak A, West SC. Visualisation of human rad52 protein and its complexes with hRad51 and DNA. *J Mol Biol*. 1998;284(4):1027–1038.
- Vu TV, Das S, Nguyen CC, Kim J, Kim JY. Single-strand annealing: molecular mechanisms and potential applications in CRISPR-Cas-based precision genome editing. *Biotechnol J*. 2022;17(7): e2100413.
- Wei DS, Rong YS. A genetic screen for DNA double-strand break repair mutations in *Drosophila*. *Genetics*. 2007;177(1):63–77.
- Yusufzai T, Kadonaga JT. HARP is an ATP-driven annealing helicase. *Science*. 2008;322(5902):748–750.

Communicating editor: B. Calvi